Chemical Engineering Journal 151 (2009) 351–358

Contents lists available at ScienceDirect

Chemical Engineering Journal

journal homepage: www.elsevier.com/locate/cej

An operability level coefficient (*OLC*) as a useful tool for correlating the performance of membrane reactors

S. Ted Oyama*, Hankwon Lim

Environmental Catalysis and Nanomaterials Laboratory, Department of Chemical Engineering (0211), Virginia Polytechnic Institute & State University, Blacksburg, VA 24061, United States

ARTICLE INFO

Article history:
Received 11 January 2009
Received in revised form 2 April 2009
Accepted 3 April 2009

Keywords:
Operability level coefficient
Damköhler number
Peclet number
Reforming
Hydrogen
Yield enhancement
Conversion enhancement
Correlation
Modeling
Simulation

ABSTRACT

An operability level coefficient (*OLC*), defined as the ratio of product permeation and product formation rates, and related to the inverse combination of the Damköhler number and the Peclet number (1/*DaPe*), is suggested as a useful tool for estimating performances of membrane reactors (MRs) operating as separators in equilibrium-limited reactions. The *OLC*s for product hydrogen formation in previously reported MRs for methane dry-reforming (MDR), methane steam-reforming (MSR), methanol steam-reforming (MeOHSR), and ethanol steam-reforming (EtOHSR) were correlated with conversion and yield enhancements. For values of *OLC*s ranging from 0.03 to 0.78, a clear universal trend for increasing conversions and hydrogen yields with increasing *OLC* was observed for these different types of reforming reactions. The *OLC* curve calculated from a numerical simulation without adjustable parameters was found to closely approximate experimental data obtained from the MRs, and was shown not to depend on the assumed kinetics. This study confirms that hydrogen selectivity (from the ratio of single-gas permeances) has a substantial influence on conversion and hydrogen yield enhancements in a MR, and demonstrates that a hydrogen selectivity of 100 is sufficient to achieve high performance in a MR.

1. Introduction

Studies of packed-bed membrane reactors (MRs) combining catalytic reactions and separation have been carried out extensively for equilibrium-limited reactions, and improvements have been demonstrated in reactant conversions and product yields compared to packed-bed reactors (PBMRs). This has been particularly studied recently for reforming reactions that produce hydrogen such as methane dry-reforming (MDR) [1–3], methane steam-reforming (MSR) [4–8], methanol steam-reforming (MeOHSR) [9–11], and ethanol steam-reforming (EtOHSR) [12,13].

Kikuchi has proposed [14,15] that a membrane used in a MR should have three important properties: high permeability, high selectivity, and stability, and suggested that for hydrogen-producing reactors the hydrogen permeation rate through the membrane should be comparable to the hydrogen formation rate for better performance in the MR. Dixon has pointed out that, in general, the reaction rate, the permeation rate, and the reactant feed rate should be matched [16]. The effect of many parameters, such as temperature, pressure, space velocity, and sweep gas flow rate [17–19], as well as permeation rate and reaction rate [20] on the performance of MRs have been considered. It has also been recognized in MR theory that two dimensionless groups, the Damköhler number (*Da*) and the Peclet number (*Pe*) are important for governing reactor behavior in isothermal [16,21] and non-isothermal [21–23,] operation, the latter in conjunction with the Stanton number. The inverse of the product of the two groups (1/*DaPe*) is a measure of the ratio of the permeation rate and the reaction rate (called the rate ratio δ by Mohan and Govind [21]), but despite its theoretical importance, it has not been used extensively to explain actual reactor behavior. Its use has been restricted to single reactions and it has not been employed across reactor systems.

This work presents a general parameter, the operability level coefficient (*OLC*), which can be used to correlate the performance of diverse membrane reactors. First, a general discussion of reactor theory is presented that describes the role of the Damköhler and Peclet numbers in MRs and explains their limitations. The *OLC* is shown to be related to the quantity (1/*DaPe*) which represents the ratio of the maximum permeation rate to the maximum reaction rate as generally obtained at feed conditions, but the *OLC* is evaluated at reaction conditions, so as will be shown, is easier to calculate. Second, the use of the *OLC* is shown to produce general correlations between conversion and yield enhancements for a variety of hydrogen-producing reactions [2–11,13]. Third, a MR model is used to reproduce the correlation curve, and to demonstrate that it is independent of the kinetic form of the rate

* Corresponding author. Tel.: +1 540 231 5309; fax: +1 540 231 5022.
E-mail address: oyama@vt.edu (S.T. Oyama).

1385-8947/$ – see front matter © 2009 Elsevier B.V. All rights reserved.
doi:10.1016/j.cej.2009.04.017

Nomenclature

A_c cross-sectional area of bed (m^2)
A_m area of membrane (m^2)
d reactor diameter (m)
$Da = (A_c L \rho_{cat} k P_{tot})/F_{tot}$ Damköhler number (ratio of reaction rate to reactant feed rate) dimensionless
D_A Fick's diffusion coefficient for reactant A ($m^2\ s^{-1}$)
$1/DaPe = (Q_i A_m)/A_c L \rho_{cat} k$ inverse *DaPe* product (ratio of permeation rate to reaction rate) dimensionless
F_A molar flow rate of species A on retentate (shell) side ($mol\ s^{-1}$)
F_A^O inlet molar flow rate of species A on retentate (shell) side ($mol\ s^{-1}$)
F_{Ar} molar flow rate of argon on tube (permeate) side ($mol\ s^{-1}$)
F_C^O inlet molar flow rate of species C on retentate (shell) side ($mol\ s^{-1}$)
F_i molar flow rate of species i on retentate (shell) side ($mol\ s^{-1}$)
F_i^{sweep} molar flow rate of species i on permeate (sweep) side ($mol\ s^{-1}$)
F_{tot} total molar flow rate (retentate) side ($mol\ s^{-1}$)
F_{tot}^{sweep} total molar flow rate on tube (permeate) side ($mol\ s^{-1}$)
k reaction rate constant ($mol\ g^{-1}\ s^{-1}\ atm^{-1}$)
k_o volumetric rate constant at inlet conditions ($mol\ s^{-1}\ m^{-3}$)
k_1 reaction rate constant of reaction 1 ($mol\ s^{-1}\ g^{-1}\ atm^{0.5}$)
k_2 reaction rate constant of reaction 2 ($mol\ s^{-1}\ g^{-1}\ atm^{-1}$)
k_3 reaction rate constant of reaction 3 ($mol\ s^{-1}\ g^{-1}\ atm^{0.5}$)
K_{CH_4} adsorption equilibrium constant of CH_4 (atm^{-1})
K_{CO} adsorption equilibrium constant of CO (atm^{-1})
K_{H_2} adsorption equilibrium constant of H_2 (atm^{-1})
K_{H_2O} adsorption equilibrium constant of H_2O (atm^{-1})
$K_{H_2}^P$ permeability constant of H_2 ($mol\ m^{-2}\ g^{-1}\ s^{-1}\ atm^{-1}$)
K_i^P permeability constant of species i ($mol\ m^{-2} g^{-1}\ s^{-1} atm^{-1}$)
K_1 equilibrium constant of reaction 1 (atm^2)
K_2 equilibrium constant of reaction 2
L catalyst bed length (m)
P_{tot} total pressure on retentate (shell) side (atm)
P_{tot}^{sweep} total pressure on permeate (sweep) side (atm)
$Pe = F_{tot}/(Q_i A_m P_{tot})$ Peclet number (ratio of reactant feed rate to permeation rate) dimensionless
Q_i permeance of species i ($mol\ m^{-2}\ s^{-1}\ Pa^{-1}$)
r_i reaction rate equation of reaction i ($mol\ s^{-1}\ g^{-1}$)
R_i^P permeation rate equation of species i ($mol\ s^{-1}\ g^{-1}$)
R gas constant ($8.314\ J\ mol^{-1}\ K^{-1}$)
R_o outer radius of reactor (m)
R_1 inner radius of reactor (m)
t thickness of membrane (m)
T reactor temperature (K)
$Y_i = F_i/F_{tot}$ dimensionless molar flow rate of species i on retentate side
$Y_i^{sweep} = F_i^{sweep}/F_{tot}^{sweep}$ dimensionless molar flow rate of species i on permeate side
Z dimensionless length of bed

Greek letters
α_i hydrogen selectivity of species i
ρ_{cat} catalyst density ($g\ m^{-3}$)
ψ catalyst loading

expression, explaining its ability to correlate results from widely different reactions.

2. Results and discussion

In the analysis of membrane reactors two groups of constants appear that have the form of Damköhler and Peclet numbers, and it is instructive to review how they originate. Although several mathematical descriptions are available in the literature, these are for specific cases [24–27]. A general derivation will be presented here, considering a very simple situation, to show that the solution will be different depending on the reaction kinetics, the geometry of the MR, and the functional form of the permeation equation. As will be argued, this puts limitations on the use of the *Da* and *Pe* numbers, and suggests the need of a more practical approach.

Considering a catalytic packed-bed membrane reactor where the catalyst bed is contiguous with the membrane and a sweep stream is used in the permeate side, the design equation for isothermal, steady-state conditions without radial gradients is:

$$\frac{dF_i}{dW} = r_i - R_i^P \tag{1}$$

where F_i is the molar flow of species i, W is the weight of catalyst, r_i is the specific rate of production of species i by reaction, and R_i^P is the specific rate of permeation of species i out of the catalyst bed. It will be assumed that the rate follows first-order kinetics, $r_i = -kP_i = -k(F_i/F_{tot})P_{tot}$, where k is the rate constant, P_i is the partial pressure, F_{tot} is the total molar flow rate, and P_{tot} is the total pressure, all on the retentate (bed) side. It will also be assumed that the rate of permeation is linear in partial pressure difference:

$$R_i^P = K_i^P A_m (P_i - P_i^{sweep}) \tag{2}$$

$$R_i^P = K_i^P A_m \left[\frac{F_i}{F_{tot}} P_{tot} - \frac{F_i^{sweep}}{F_{tot}^{sweep}} P_{tot}^{sweep} \right] \tag{3}$$

where K_i^P is the specific permeability constant, A_m is the membrane area, and P_i^{sweep}, F_i^{sweep}, F_{tot}^{sweep} and P_{tot}^{sweep} are the partial pressure, molar flow rate, total molar flow rate, and total pressure in the permeate (sweep) stream. The permeability constant is the permeance divided by the weight of the catalysts (Q_i/W). Using the fact that the differential catalyst weight, dW, is given by the product of the cross-sectional area of the bed, A_c, the bed length, L, the catalyst bed density, ρ_{cat}, and the differential dimensionless length of the bed, dZ, $dW = A_c L \rho_{cat} dZ$, and substituting this expression into the design Eq. (1) gives, after simple manipulation, the following expression which assumes the total pressure on the bed and sweep side are the same:

$$\frac{dF_i}{dZ} = A_c L \rho_{cat} k P_{tot} \left[-\frac{F_i}{F_{tot}} - \frac{K_i^P A_m}{k} \left(\frac{F_i}{F_{tot}} - \frac{F_i^{sweep}}{F_{tot}^{sweep}} \right) \right] \tag{4}$$

This expression can be expressed in dimensionless form by defining dimensionless molar flow rates based on the total inlet molar flow rate $Y_i = \frac{F_i}{F_{tot}}$ and $Y_i^{sweep} = \frac{F_i^{sweep}}{F_{tot}^{sweep}}$:

$$\frac{dY_i}{dZ} = Da \left[-Y_i - \frac{1}{DaPe} \left(Y_i - Y_i^{sweep} \right) \right] \tag{5}$$

The equation uses the parameters *Da* and *Pe* defined as follows:

$$Da = \frac{A_c L \rho_{cat} k P_{tot}}{F_{tot}} \quad (6)$$

$$Pe = \frac{F_{tot}}{Q_i A_m P_{tot}} \quad (7)$$

As has been recognized in the literature [16], these groups consist of ratios of important rates that govern the performance of the reactor: the rate of reaction, the rate of reactant feed, and the rate of permeation. For example, the Damköhler number is given by *Da* = (reactor volume) (maximum rate per volume)/(inlet flow rate), and the Peclet number is given by *Pe* = (inlet flow rate)/(maximum permeation rate per volume) (reactor volume). A derived quantity is the inverse Damköhler–Peclet product, 1/*DaPe* = (maximum permeation rate per volume)/(maximum reaction rate per volume):

$$1/DaPe = \frac{Q_i A_m}{A_c L \rho_{cat} k} \quad (8)$$

It should be recalled that these equations were derived with a number of simplifying assumptions, namely that no radial gradients were present, that the reaction rate was first-order, that the permeation rate was linear in pressure difference, and that the total pressure in the reactant and permeate sides were the same. Deviations from these assumptions complicate the equations and can render them incapable of yielding succinct solutions. Even in relatively simple cases they require particular treatments, which yield different expressions for *Da* and *Pe*. For example, for series reactions, A → R → S, not constrained to equal pressures across the membrane [25], the solution of the mole balance equation with the catalyst on the tube side gives $Da = (\pi d^2 L k_1 P_{tot})/4F_A^o RT$ and $1/DaPe = -(8D_A)/d^2 k_1 \ln(d/d + 2t)$, where d is the reactor diameter, k_1 is the rate constant of the first reaction, F_A is the inlet molar flow of the first reactant, D_A is the Fick's diffusion coefficient of the first reactant, and t is the thickness of the membrane. For series-parallel reactions A + B → R + T and R + B → S + T [25] a similar treatment gives $Da = (\pi d^2 L k_1/4F_A^O)/(P_{tot}/RT)^2$ and $1/DaPe = -(8D_A RT)/d^2 k_1 P_{tot} \ln(d/d + 2t)$. For a dehydrogenation reaction with the catalyst on the annular shell side, A → B + C [26], the following expressions are reported, $Da = (\pi(R_o^2 - R_i^2) L \psi k_o P_{tot})/F_C^O$ and $1/DaPe = (2R_i Q_C)/(R_o^2 - R_i^2)\psi k_o$, where R_o and R_i are the outer and inner radii of the reactor, ψ is the catalyst loading, k_o is the volumetric rate constant at inlet conditions, F_C^O is the molar feed rate of the permeating species C, and Q_C is the permeability of the species. For another dehydrogenation reaction the following expression is given $1/DaPe = (QP^{0.5}A)/k_r V$, where Q is the permeance, P is the reactor pressure, A is the membrane surface area, k_r is the reaction rate constant (mol m^{-3} Pa^{-1} s^{-1}), and V is the catalyst volume [27,28]. Although, the elements of these equations are similar to those presented in Eqs. (7) and (9), the detailed forms are different.

The design parameters (*Da* and 1/*DaPe*) have been used to explain the behavior of membrane reactors, always concentrating on a specific system For example optimum levels of *Da* and *DaPe* to maximize product yield have been plotted for a general paraffin dehydrogenation reaction [29], and *Da* and *Pe* for the cyclohexane dehydrogenation reaction [26], where conversion has been shown to increase with high (1/*DaPe*) for the same dehydrogenation reaction [27]. One limitation for generality is that the values of these parameters, particularly 1/*DaPe*, vary according to their definition. For example in one study *Da* ranged from 1×10^{-2} to 1×10^{3} and 1/*DaPe* from 1×10^{-4} to 1×10^{4} [29], in another *Da* varied from 1 to 10^4 and 1/*DaPe* from 1×10^{-8} to 1×10^{4} [26], and in still another 1/*DaPe* took on values between 0 and 1 [27].

The range of 0–1 for 1/*DaPe* = (permeation rate/reaction rate) is reasonable since it is expected that the permeation rate will not exceed the reaction rate, and this is the range of *OLC* for the work reported here. However, if the parameters are defined at entrance conditions, the range can certainly be exceeded. As explained by Lund and co-workers, experimentally, the Damköhler number can be varied by increasing or decreasing the reactor volume (or equivalently the contact time, as will be done in this paper later), and *DaPe* by altering the membrane area per reactor volume (e.g., shell with multiple tubes) [29].

An attractive attribute of these dimensionless parameters is that they contain fundamental quantities (such as rate constants and permeability coefficients), and essential reactor design variables such as volume ($A_c L$) and membrane area (A_m). They also utilize initial conditions (F_{tot}, P_{tot}) and these give rise to the maximum rates that were noted earlier. A difficulty in the application of dimensionless groups is that they need to be derived for each particular case. In addition as shown for the *Da* and (1/*DaPe*) numbers, the values of these groups are not unique as they contain aspects about the reactor geometry and the reaction stoichiometry. And although the presence of fundamental quantities like rate constants and permeability coefficients or diffusivities give elegance and conciseness to the equations, these quantities are not always readily available. It would be useful to have a quantity that could be readily accessible from experimental measurements. The operability level coefficient is introduced here with this attribute.

The operability level coefficient is defined as the ratio of the actual permeation rate and the actual formation rate of a critical product in a membrane reactor. The critical product is usually the one for which the membrane is permselective. The product formation rate is the total production rate, including that which permeates.

$$OLC = \frac{(\text{product permeation rate})}{(\text{product formation rate})} = \frac{(\text{permeance})(\text{area})(\Delta P)}{(\text{rate})(\text{volume})} \quad (9)$$

The *OLC* may also be defined in terms of the *Da* and *Pe* numbers, but evaluated at reaction conditions.

$$OLC = (1/DaPe)_{\text{reaction conditions}} \quad (10)$$

Conversion and product yield enhancements were defined from quantities obtained experimentally in MRs and PBRs.

$$\text{Conversion enhancement (\%)} = \frac{\text{conversion (MR)} - \text{conversion (PBR)}}{\text{conversion (PBR)}} \times 100 \quad (11)$$

$$\text{Product yield enhancement (\%)} = \frac{\text{product yield (MR)} - \text{product yield (PBR)}}{\text{product yield (PBR)}} \times 100 \quad (12)$$

A literature survey was carried out to review results of previously reported MRs for different reforming reactions such as MDR, MSR, MeOHSR, and EtOHSR, and to obtain the *OLC*. Table 1 summarizes the performances of the reported MRs for the reforming reactions. For the calculation of the *OLC* from Pd membrane data, the actual pressures on the retentate and permeate side were used and converted to $P^{1/2}$. Lee et al. [2] and Irusta et al. [3] carried out the MDR reaction with supported Rh catalysts at 873 and 823 K and 1 atm in MRs fitted with silica and palladium membranes, respectively. Conversion enhancements of 56% and 18% were obtained in the MRs with respective *OLC*s of 0.68 and 0.17. Hacarlioglu et al. [4], Tsuru et al. [5], and Tong and Matsumura [6] performed the MSR reaction with supported Ni catalysts at 773 K (1–20 atm), 773 K (1 atm), and 800 K (1 atm), respectively, and in MRs equipped with silica and palladium membranes with hydrogen permeances of 1–2 × 10^{-7} mol m^{-2} s^{-1} Pa^{-1}. Conversion enhancements of 27 (773 K), 82 (773 K), 11–34% (800 K) were obtained in the MRs with respective *OLC*s of 0.40, 0.73 and 0.23–0.54. Tong and Matsumura

Table 1
Summary of performances in previously reported MRs.

Reforming reaction	T (K)	Catalyst	Membrane H_2 permeance (mol m^{-2} s^{-1} Pa^{-1})	Selectivity	Operability level coefficient (*OLC*)	X (PBR) (%)	ΔX[c] (%)	H_2[d] (%)
$CH_4 + CO_2$ [2]	873	Rh/Al_2O_3 0.04 g	Silica 3×10^{-7}	H_2/CH_4 300	0.68	34	56	78
$CH_4 + CO_2$ [3]	823	Rh/La_2O_3–SiO_2 0.05 g	Pd/Ag NR[a]	NR[a]	0.17[e]	28	18	NR[a]
$CH_4 + H_2O$ [4]	773	$Ni/MgAl_2O_4$ 2 g	Silica 1×10^{-7}	H_2/CH_4 700	0.40	44	27	35
$CH_4 + H_2O$ [5][b]	773	Ni/Al_2O_3 0.25 g	Silica 2×10^{-7}	H_2/N_2 70	0.73	44	82	NR[a]
$CH_4 + H_2O$ [6][b]	800	Ni/Al_2O_3 NR[a]	Pd 2×10^{-7}	H_2/Ar 2000	0.23–0.54	53	11–34	NR[a]
$CH_4 + H_2O$ [7][b]	773	Ni/Al_2O_3 NR[a]	Pd $1–3 \times 10^{-6}$	H_2/Ar 2000	0.25–0.78	44	21–82	NR[a]
$CH_4 + H_2O$ [7][b]	823	Ni/Al_2O_3 NR[a]	Pd 2×10^{-6}	H_2/Ar 2000	0.23–0.52	61	15–36	NR[a]
$CH_4 + H_2O$ [8]	823	Noble metal 50 g	Pd NR[a]	∞	0.57–0.74[f]	45–56	27–53	31–58
$CH_3CHO + H_2O$ [9]	493	$CuO/ZnO/Al_2O_3$ 7.5 g	Pd/Ag 1×10^{-7}	∞	0.11	38	16	18
$CH_3CHO + H_2O$ [9]	523	$CuO/ZnO/Al_2O_3$ 7.5 g	Pd/Ag 2×10^{-7}	∞	0.15	43	19	29
$CH_3CHO + H_2O$ [10]	723	Ni/Al_2O_3 0.25 g	Pd/Ag NR[a]	NR[a]	0.50[g]	NR[a]	NR[a]	33
$CH_3CHO + H_2O$ [11]	473	Pt/SiO_2 5 g	Silica 7×10^{-8}–5×10^{-7}	∞	0.03–0.10	63–66	2–5	NR[a]
$C_2H_5OH + H_2O$ [13]	623	Co–Na/ZnO 0.6 g	Silica $5–7 \times 10^{-8}$	H_2/CO_2 200–600	0.13–0.16	50	12–16	8–22
$C_2H_5OH + H_2O$ [13]	623	Co–Na/ZnO 0.6 g	Pd/Cu 5×10^{-7}–4×10^{-6}	H_2/CO_2 700–1000	0.38–0.58	50	26–44	43–69

[a] NR: not reported.
[b] Reactant conversions and hydrogen yields at equilibrium were used for enhancement calculations because no experimental data in PBRs were provided.
[c] Enhancement in conversion.
[d] Enhancement in H_2 yield.
[e] $R_{CH_4}/R_{H_2\ permeation}$ was provided.
[f] Separation factor (permeated H_2/total H_2) was provided.
[g] H_2 removal ratio (permeated H_2/produced H_2) was provided.

[7] also studied the MSR reaction with commercial nickel catalysts at 773 and 823 K at 1 atm in MRs fitted with palladium membranes with hydrogen permeances of $1–3 \times 10^{-6}$ mol m^{-2} s^{-1} Pa^{-1}. Conversion enhancements in the range of 15–82% were obtained in the MRs with *OLC*s in the range of 0.23–0.78. Patil et al. [8] carried out the MSR reaction with a noble metal catalyst at 823 K at 2 atm in a MR containing a palladium-based membrane and conversion enhancements in the range of 27–53% and hydrogen yield enhancements in the range of 31–58% were obtained in the MR with *OLC*s in the range of 0.57–0.74. Basile et al. [9], Kikuchi et al. [10], and Lee et al. [11] investigated the MeOHSR reaction with $CuO/ZnO/Al_2O_3$, Ni/Al_2O_3, and Pt/SiO_2 catalysts at 493–523 K (1 atm), 723 K (1 atm), and 473 K (1 atm), respectively, and in MRs equipped with palladium and silica membranes with hydrogen permeances of 7×10^{-8}–5×10^{-7} mol m^{-2} s^{-1} Pa^{-1}. Conversion enhancements in the range of 2–19% and hydrogen yield enhancements in the range of 18–33% were obtained in the MRs with *OLC*s in the range of 0.03–0.50. Lim et al. [13] studied the EtOHSR reaction with a Co–Na/ZnO catalyst at 623 K and 1 atm in MRs fitted with silica and palladium membranes with hydrogen permeances of 10^{-8}–10^{-6} mol m^{-2} s^{-1} Pa^{-1}. Conversion enhancements of 12%, 16%, 26%, and 44% and hydrogen yield enhancements of 8%, 22%, 43%, and 69% were obtained in the MRs with respective *OLC*s of 0.13, 0.16, 0.38 and 0.58. The results, together with the reaction conditions and the membrane dimensionless, are summarized in Table 1.

The previous examples show that different types of reforming reactions have been carried out in MRs and improved reactant conversions in the range of 2–82% and hydrogen yields in the range of 8–78% were obtained in the MRs. These enhancements in the MRs were possible because the continuous removal of hydrogen during the reactions shifted the equilibria to the products. From the MR studies for the MSR reaction, it was found that there were significant differences in the conversion enhancement (11–82%) in the MRs fitted with membranes with similar hydrogen permeances of $1–2 \times 10^{-7}$ mol m^{-2} s^{-1} Pa^{-1}. The reason for this can be found in their different *OLC*s, with the highest conversion enhancement of 82% obtained in a MR with the highest *OLC* of 0.73. An obvious trend for higher conversion and hydrogen yield enhancements with higher *OLC* was observed for all reforming reactions presented in Table 1.

In the present work different reforming reactions were studied to find a general relationship between *OLC* and MR performance. Fig. 1 shows that increasing conversion enhancement was observed

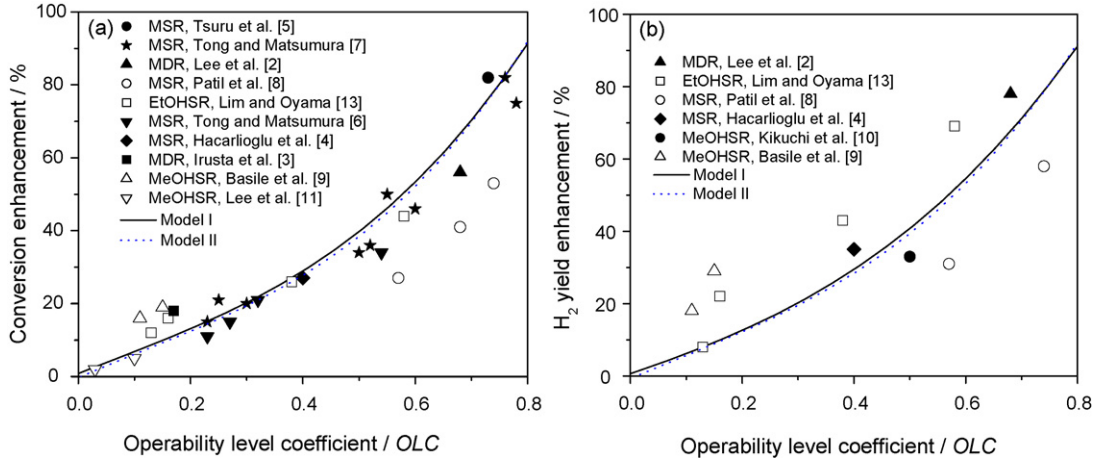

Fig. 1. Operability level coefficient (*OLC*) and enhancement of conversion and yield in the MRs.

with increasing *OLC*. The solid line is the *OLC* curve of calculated conversion enhancements obtained from a one-dimensional mathematical simulation developed to describe the performance of the MSR reaction at 773 K in a MR. This temperature was chosen because it was in the middle of temperatures used in the reforming reactions. The reaction rate expressions were obtained from Xu and Froment [30] and will be referred to as Model I. The constants are given in Appendix A. The fit is good and gives a variance of $\sigma^2 = 56$ and a coefficient of regression of $R^2 = 0.88$.

$$CH_4 + H_2O \rightleftarrows CO + 3H_2 \quad \Delta H^o_{298} = 206\ \text{kJ mol}^{-1} \tag{13}$$

$$CO + H_2O \rightleftarrows CO_2 + H_2 \quad \Delta H^o_{298} = -41\ \text{kJ mol}^{-1} \tag{14}$$

$$CH_4 + 2H_2O \rightleftarrows CO_2 + 4H_2 \quad \Delta H^o_{298} = -165\ \text{kJ mol}^{-1} \tag{15}$$

$$r_1 = \frac{k_1(P_{CH_4}P_{H_2O}/P_{H_2}^{2.5} - P_{H_2}^{0.5}P_{CO}/K_1)}{\text{DEN}^2}$$

$$r_2 = \frac{k_2(P_{CO}P_{H_2O}/P_{H_2} - P_{CO_2}/K_2)}{\text{DEN}^2}$$

$$r_3 = \frac{k_3(P_{CH_4}P_{H_2O}^2/P_{H_2}^{3.5} - P_{H_2}^{0.5}P_{CO_2}/K_1K_2)}{\text{DEN}^2} \tag{16}$$

$$\text{DEN} = 1 + K_{CO}P_{CO} + K_{H_2}P_{H_2} + K_{CH_4}P_{CH_4} + K_{H_2O}(P_{H_2O}/P_{H_2}) \tag{17}$$

The reactions comprise the reforming reaction to form CO Eq. (13), the water gas-shift reaction Eq. (14), and the reforming reaction to produce CO_2 Eq. (15). In the simulation it was assumed that the membrane used in the MR had infinite selectivity to hydrogen, with selectivity obtained from the ratio of single-gas permeances. The reactor modeling used a conventional one-dimensional treatment using molar flow rates, and details are provided in Appendix B. The *OLC* curve from the numerical simulation showed a close match with experimental data with only minor deviations.

Fig. 1 also shows that increasing hydrogen yield enhancement was obtained with increasing *OLC*. The solid line is the *OLC* curve of calculated hydrogen yield enhancements obtained from the numerical simulation, and again a good fit to the experimental data was obtained with a variance of $\sigma^2 = 180$ and a coefficient of regression of $R^2 = 0.81$. The correspondence between the calculated *OLC* curves and the experimental data motivated us to investigate whether the results were general or dependent on the kinetics of the reactions. The calculated *OLC* curves in Fig. 1 were obtained from the kinetic equations Eqs. (17) and (18) reported by Xu and Froment [30] with 9 parameters (3 rate constants, 2 equilibrium constants, and 4 adsorption equilibrium constants). An additional description was obtained by fitting the kinetic data of Xu and Froment [30] to a simple model denoted as Model II that simplified both the chemical reactions involved and the kinetic expressions. Model II considers only Eqs. (1) and (2) (the main reforming reaction and the water gas-shift reaction) and describes them with rate expressions of the form of the law of mass action Eq. (18). The parameters are given in Appendix C. With a much smaller set of fitting parameters (4 vs. 9), Model II gives a worse fit to the data. Nevertheless, the simulated *OLC* curves from Model II were in excellent agreement with those from Model I for both conversion and hydrogen yield enhancements (dotted lines in Fig. 1). This comparison demonstrates that the results are largely independent of kinetics. The calculated *OLC* curves fit data from many different systems at different conditions because the important quantities considered are the measured reaction rates and permeance, and these are global quantities not dependent on the kinetics of the reaction.

The one-dimensional simulation used here does not consider radial gradients. The relatively small deviations observed between the data and the calculated curves (Fig. 1) may be due to effects due to radial diffusion, or temperature, as noted earlier, or membrane selectivity, as will be discussed later. Radial diffusion would tend to give lower conversion and yield enhancement because concentration polarization effects would tend to reduce the driving force for permeance. Higher temperature would tend give higher conversion and yield enhancements for endothermic hydrogen production reactions.

The fact that the correlation appears to be a phenomenon that is related to global quantities led us to explore further the basis of the correlation. The product formation rates and permeation rates can be varied not only by considering different reactions but by analyzing data from a single reactor. This can be done by taking values at different locations down the length of the reactor, or equivalently by varying the contact time. The latter approach was taken here. The *OLC* and enhancements in a MR were simulated for different contact times using the same reactor analysis used for Model I by varying inlet flow rate (F_{CH_4}) and maintaining hydrogen permeance the same (Table 2). Fig. 2a and b shows that increasing enhancements were observed with increasing contact time. Fig. 2c and d show the *OLC* curve obtained from Model I and enhancement data obtained from the simulation for different contact times. Identical results were obtained, indicating that indeed the global nature of the permeation rate and product formation rate were producing the correlation.

The analysis so far has not considered membrane selectivity. It has been assumed in the preceding analysis that the selectivity was infinite, justified because the studies were carried out with Pd and silica-based membranes [31–38] which mostly have excellent selectivity for hydrogen (Table 1).

To study the effect of hydrogen selectivity on reactant conversion and hydrogen yield enhancements, *OLC* curves were obtained from the simulation by varying the H_2/CH_4 selectivity from 3 (Knudsen diffusion selectivity) to ∞ with a constant hydrogen permeance (Fig. 3). With the assumption of Knudsen diffusion selectivity ($H_2/H_2O = 3$, $H_2/CO = 4$, and $H_2/CO_2 = 5$), it was found that lower conversion and hydrogen yield enhancements were obtained compared to those obtained with the membrane with infinite hydrogen selectivity. This is reasonable because some of the product passes through the membrane, which decreases product yields and some of the reactant escapes the reaction zone, which decreases reaction

Table 2
Enhancement of conversion and yield over contact time in MRs.

F_{CH_4} (mol s^{-1})	Contact time (s)	*OLC*	Conversion enhancement (%)	H_2 yield enhancement (%)
3.0×10^{-4}	3	0.01	1	1
1.5×10^{-5}	5.4	0.11	7	4
5.0×10^{-6}	16	0.30	20	20
3.4×10^{-6}	24	0.40	29	29
2.0×10^{-6}	41	0.57	48	50
1.7×10^{-6}	48	0.62	57	55
1.3×10^{-6}	60	0.70	71	73

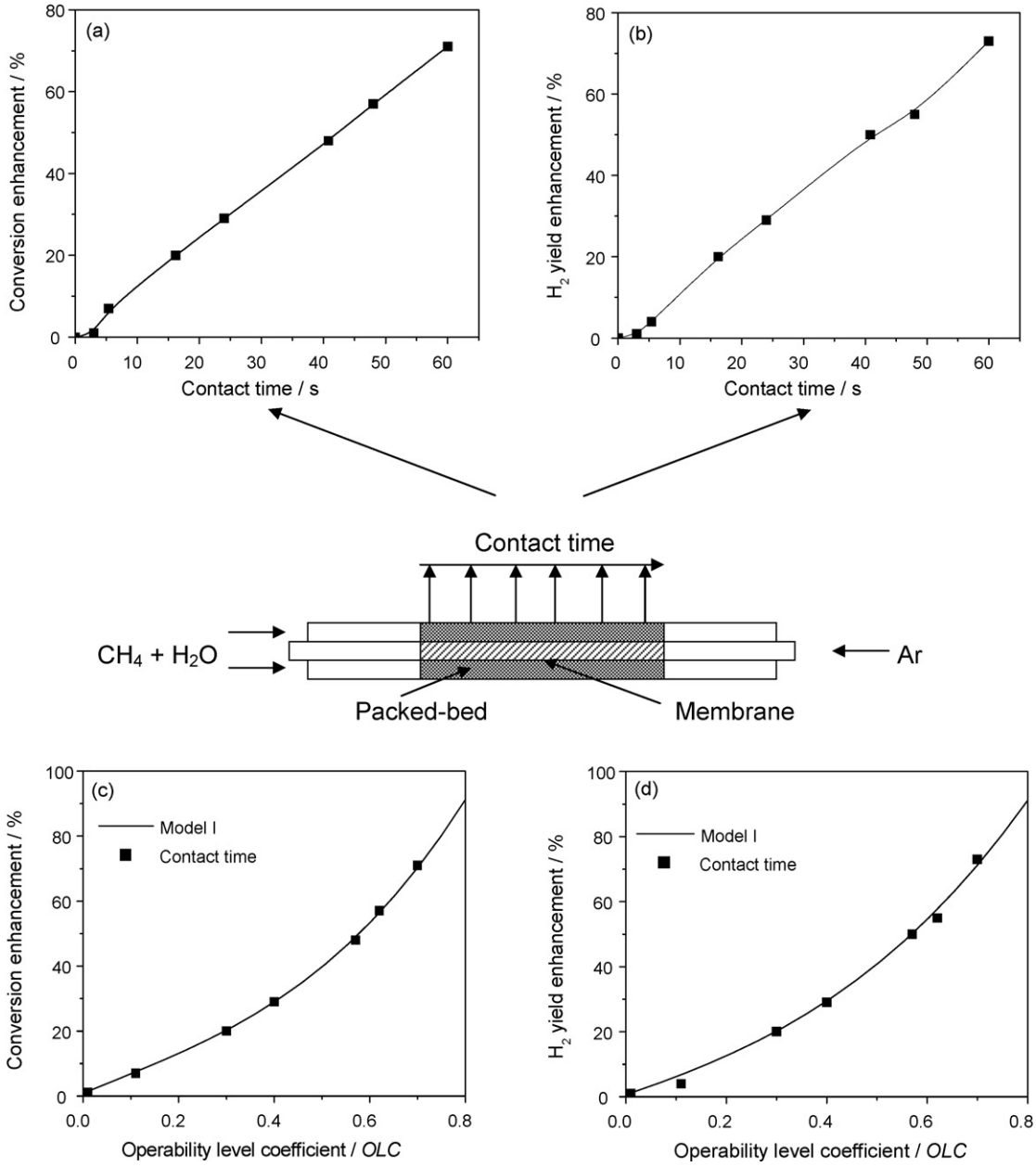

Fig. 2. Effect of contact time in MRs.

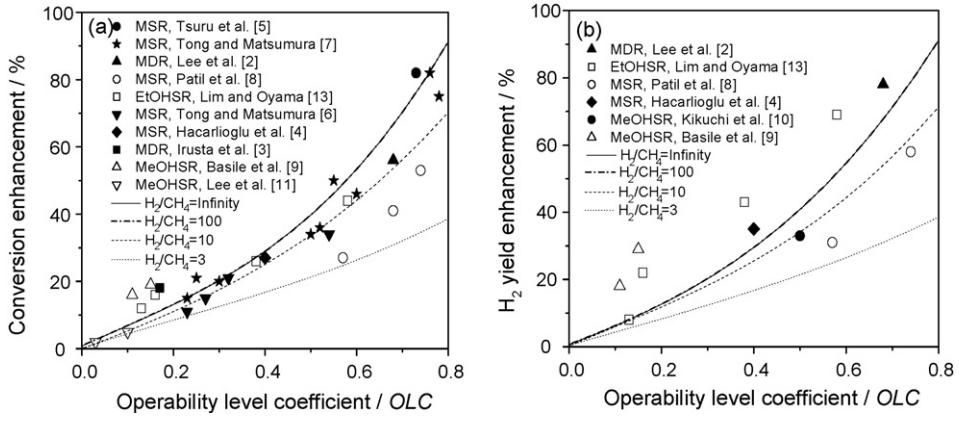

Fig. 3. Effect of hydrogen selectivity on enhancement of conversion and yield in MRs.

rate. With increasing hydrogen selectivity, it was found that higher conversion and hydrogen yield enhancements were obtained and a membrane with a H_2/CH_4 selectivity of 100 showed essentially the same results as obtained with the membrane with ∞ hydrogen selectivity (Fig. 3). These simulation results also verify experimental results by Lim et al. [13] who reported that for membranes with similar permeance (7×10^{-8} and 5×10^{-8} mol m^{-2} s^{-1} Pa^{-1}) the membrane with higher H_2/CH_4 selectivity (350 vs. 60) showed a higher hydrogen yield enhancement (15% more). It can be concluded from these results that membranes with higher hydrogen selectivity give better performance in a MR and that a H_2/CH_4 selectivity of 100 can be considered as a criterion for a membrane to achieve high performance in a MR.

To summarize, a clear trend for increasing reactant conversion and product yield enhancements with increasing *OLC* was observed in the MRs, and this relationship was found to be generally applicable to different types of reforming reactions. These results indicate that the best MR performance is obtained as *OLC* approaches 1, namely when reaction rate and permeance are comparable, as noted earlier [14–16]. The *OLC* curve obtained from the numerical simulation was found to fit the experimentally obtained data. The numerical simulations used results from a specific system (MSR) but are likely generally applicable to other reforming reactions because the analysis focuses on observable system quantities (permeance and reaction rates) and not on the kinetics of the reaction. The results are important because they allow the correlation of MR performance from knowledge of the reaction rate and the permeance of the membrane.

3. Conclusions

An operability level coefficient defined as the ratio of product permeation and product formation rates was proposed as a means for estimating the performance of membrane reactors. Conversion enhancements ranging from 2% to 82% and hydrogen yield enhancements ranging from 8% to 78% were obtained with *OLC*s ranging from 0.03 to 0.78 from previously reported MRs for different hydrogen-forming reactions (methane dry-reforming, methane steam-reforming, methanol reforming and ethanol reforming). The effect of *OLC* on performances of the MRs was studied and increasing conversion and hydrogen yield enhancements were obtained with increasing *OLC*s to a limiting value of 1, where the rates of permeation and reaction are equal. The *OLC* curve of calculated data obtained from a one-dimensional numerical simulation was found to be a useful tool to estimate conversion and hydrogen yield enhancements in MRs at given *OLC*s. It was also demonstrated that membranes should have a hydrogen selectivity, defined as the ratio of single-gas permeances of hydrogen to other gases, of 100 to achieve the performance of a reactor with a membrane of infinite selectivity.

Acknowledgments

The authors acknowledge the Director, National Science Foundation, Division of Chemical, Bioengineering, Environmental, and Transport Systems (CBET) under grant CBET 0651238 for support of this work.

Appendix A. Kinetics parameters of Model I (Xu and Froment [30])

$$k_1 = 4.2 \times 10^{15} \exp\left(\frac{-2.4 \times 10^5}{RT}\right) \quad K_{CH_4} = 6.7 \times 10^4 \exp\left(\frac{3.8 \times 10^4}{RT}\right)$$

$$k_2 = 2.0 \times 10^6 \exp\left(\frac{-6.7 \times 10^4}{RT}\right) \quad K_{CO} = 8.2 \times 10^5 \exp\left(\frac{7.1 \times 10^4}{RT}\right)$$

$$k_3 = 1.0 \times 10^{15} \exp\left(\frac{-2.4 \times 10^5}{RT}\right) \quad K_{H_2} = 6.1 \times 10^9 \exp\left(\frac{8.3 \times 10^4}{RT}\right)$$

$$K_1 = \exp\left(\frac{-2.7 \times 10^4}{T} + 30.114\right) \quad K_{H_20} = 1.8 \times 10^5 \exp\left(\frac{8.9 \times 10^4}{RT}\right)$$

$$K_2 = \exp\left(\frac{4.4 \times 10^3}{T} - 4.036\right)$$

Appendix B. One-dimensional reactor model

$$\frac{dF_{CH_4}}{dW} = -r_1 - r_3 \quad \frac{dF_{CO_2}}{dW} = r_2 + r_3$$

$$\frac{dF_{H_2O}}{dW} = -r_1 - r_2 - 2r_3 \quad \frac{dF_{H_2}}{dW} = 3r_1 + r_2 + 4r_3 - R^P_{H_2}$$

$$\frac{dF_{CO}}{dW} = r_1 - r_2 \quad \frac{dF_i^{sweep}}{dW} = r_i^{sweep}$$

$$F_{tot} = F_{CH_4} + F_{H_20} + F_{CO} + F_{CO_2} + F_{H_2}$$

$$F_{tot}^{sweep} = F_{A_r}^{sweep} + \sum F_i^{sweep}$$

$$P_{CH_4} = \left(\frac{F_{CH_4}}{F_{tot}}\right) P_{tot} \quad P_i^{sweep} = \left(\frac{F_i^{sweep}}{F_{tot}^{sweep}}\right) P_{tot}^{sweep}$$

$$P_{H_20} = \left(\frac{F_{H_20}}{F_{tot}}\right) P_{tot} \quad R^P_{H_2} = K^P_{H_2}(P_{H_2} - P^{sweep}_{H_2})$$

$$P_{CO} = \left(\frac{F_{CO}}{F_{tot}}\right) P_{tot} \quad K^P_{H_2} = \frac{Q_{H_2} A_c}{W}$$

$$P_{CO_2} = \left(\frac{F_{CO_2}}{F_{tot}}\right) P_{tot} \quad R_i = \frac{K^P_{H_2}}{\alpha_i}(P_i - P_i^{sweep})$$

$$P_{H_2} = \left(\frac{F_{H_2}}{F_{tot}}\right) P_{tot}$$

Appendix C. Parameters of Model II

$$CH_4 + H_2O \rightleftarrows CO + 3H_2 \quad \Delta H^o_{298} = 206\ \text{kJ mol}^{-1}$$

$$CH_4 + H_2O \rightleftarrows CO_2 + H_2 \quad \Delta H^o_{298} = -41\ \text{kJ mol}^{-1}$$

$$r_1 = k_4 \left(P_{CH_4} P_{H_2O} - \frac{P_{CO} {P_{H_2}}^3}{K_1}\right) \quad r_2 = k_5 \left(P_{CO} P_{H_2O} - \frac{P_{CO_2} P_{H_2}}{K_2}\right) \tag{18}$$

At $T = 773$ K; $k_4 = 5.36$ mol s^{-1} g^{-1} atm^{-2}; $k_5 = 100.00$ mol s^{-1} g^{-1} atm^{-2}; $K_1 = 0.01$ atm^2; $K_2 = 5.2$.

References

[1] A.K. Prabhu, S.T. Oyama, Highly hydrogen selective ceramic membranes: application to the transformation of greenhouse gases, J. Membr. Sci. 176 (2000) 233–248.
[2] D. Lee, P. Hacarlioglu, S.T. Oyama, The effect of pressure in membrane reactors: trade-off in permeability and equilibrium conversion in the catalytic reforming of CH_4 with CO_2 at high pressure, Top. Catal. 29 (2004) 45–57.
[3] S. Irusta, J. Munera, C. Carrara, E.A. Lombardo, L.M. Cornaglia, A stable, novel catalyst improves hydrogen production in a membrane reactor, Appl. Catal. A: Gen. 287 (2005) 147–158.

[4] P. Hacarlioglu, Y. Gu, S.T. Oyama, Studies of the methane steam reforming reaction at high pressure in a ceramic membrane reactor, J. Nat. Gas Chem. 15 (2006) 73–81.
[5] T. Tsuru, K. Yamaguchi, T. Yoshioka, M. Asaeda, Methane steam reforming by microporous catalytic membrane reactors, AICHE J. 50 (2004) 2794–2805.
[6] J. Tong, Y. Matsumura, Effect of catalytic activity on methane steam reforming in hydrogen-permeable membrane reactor, Appl. Catal. A: Gen. 286 (2005) 226–231.
[7] J. Tong, Y. Matsumura, Pure hydrogen production by methane steam reforming with hydrogen-permeable membrane reactor, Catal. Today 111 (2006) 147–152.
[8] C.S. Patil, M. van Sint Annaland, J.A.M. Kuipers, Fluidized bed membrane reactor for ultrapure hydrogen production via methane steam reforming: experimental demonstration and model validation, Chem. Eng. Sci. 62 (2007) 2989–3007.
[9] A. Basile, F. Gallucci, L. Paturzo, A dense Pd/Ag membrane reactor for methanol steam reforming: experimental study, Catal. Today 104 (2005) 244–250.
[10] E. Kikuchi, S. Kawabe, M. Matsukata, Steam reforming of methanol on Ni/Al_2O_3 catalyst in a Pd-membrane reactor, J. Jpn. Pet. Inst. 46 (2003) 93–98.
[11] D.-W. Lee, S.-E. Nam, B. Sea, S.-K. Ihm, K.-H. Lee, Preparation of Pt-loaded hydrogen selective membranes for methanol reforming, Catal. Today 118 (2006) 198–204.
[12] S.A. Birdsell, R.S. Willms, R.C. Dye, Pure hydrogen production from octane, ethanol, methanol, and methane reforming using a palladium membrane reactor, in: Proceedings of the Intersociety Energy Conversion Engineering Conference, 32, 1997, pp. 1942–1946.
[13] H. Lim, Y. Gu, S.T. Oyama, Studies of the ethanol steam reforming reaction in a membrane reactor, ACS Pet. Chem. Div. Prep. 51 (2006) 31–33.
[14] E. Kikuchi, Membrane reactor application to hydrogen production, Catal. Today 56 (2000) 97–101.
[15] E. Kikuchi, Hydrogen-permselective membrane reactors, Cattech (March) (1997) 67–74.
[16] A.G. Dixon, Recent research in catalytic inorganic membrane reactors, Int. J. Chem. Eng. 1 (2003) 1.
[17] Y.V. Gokhale, R.D. Noble, J.L. Falconer, Analysis of a membrane enclosed catalytic reactor for butane dehydrogenation, J. Membr. Sci. 77 (1993) 197–206.
[18] J. Shu, B.P.A. Grandjean, S. Kaliaguine, Asymmetric Pd-Ag/stainless steel catalytic membranes for methane steam reforming, Catal. Today 25 (1995) 327–332.
[19] J.S. Oklany, K. Hou, R. Hughes, A simulative comparison of dense and microporous membrane reactors for the steam reforming of methane, Appl. Catal. A: Gen. 170 (1998) 13–22.
[20] J.K. Ali, D.W.T. Rippin, Effect of reaction and permeation rates on the performance of a membrane reactor for methylcyclohexane dehydrogenation, Sep. Sci. Technol. 29 (1994) 2475–2492.
[21] K. Mohan, R. Govind, Effect of temperature on equilibrium shift in reactors with a permselective wall, Ind. Eng. Chem. Res. 27 (1988) 2064–2070.
[22] T.T. Tsotsis, A.M. Champagnie, S.P. Vasileaidis, Z.D. Ziaka, R.G. Minet, Packed-bed catalytic membrane reactors, Chem. Eng. Sci. 47 (1992) 2903–2908.
[23] A.G. Dixon, Analysis of intermediate product yield in distributed feed non-isothermal tubular membrane reactors, Catal. Today 67 (2001) 189–203.
[24] S. Agarwalla, C.R.F. Lund, Use of a membrane reactor to improve selectivity to intermediate products in consecutive catalytic reactions, J. Membr. Sci. 70 (1992) 129–141.
[25] L.A. Bernstein, C.R.F. Lund, Membrane reactors for catalytic series and series-parallel reactions, J. Membr. Sci. 77 (1993) 155–164.
[26] W.S. Moon, S.B. Park, Design guide of a membrane for a membrane reactor in terms of permeability and selectivity, J. Membr. Sci. 170 (2000) 43–51.
[27] S. Battersby, P.W. Teixeira, J. Beltramini, M.C. Duke, V. Rudolph, J.C. Diniz da Costa, An analysis of the Peclet and Damkohler numbers for dehydrogenation reactions using molecular sieve (MSS) membrane reactors, Catal. Today 116 (2006) 12–17.
[28] S. Tosti, A. Basile, L. Bettinalia, F. Borgognonia, F. Gallucci, C. Rizzelo, Design and process study of Pd membrane reactors, Int. J. Hydrogen Energy 33 (2008) 5098.
[29] C.M. Reo, L.A. Bernstein, C.R.F. Lund, Cocurrent membrane reactors vs. PFRs for shifting dehydrogenation equilibrium, AIChE J. 43 (1997) 495.
[30] J. Xu, G.F. Froment, Methane steam reforming, methanation and water-gas shift. I. Intrinsic kinetics, AICHE J. 35 (1989) 88–95.
[31] Y. Gu, S.T. Oyama, High molecular permeance in a pore-less ceramic membrane, Adv. Mater. 19 (2007) 1636–1640.
[32] Y. Gu, S.T. Oyama, Ultra-thin, hydrogen-selective silica membranes deposited on alumina graded structures prepared from size-controlled boehmite sols, J. Membr. Sci. 306 (2007) 216–227.
[33] H. Verweij, Y.S. Lin, J. Dong, Microporous silica and zeolite membranes for hydrogen purification, MRS Bull. 31 (2006) 756.
[34] A. Brunetti, G. Barbieri, E. Drioli, K.-H. Lee, B. Sea, D.-W. Lee, WGS reaction in a membrane reactor using a porous stainless steel supported silica membrane, Chem. Eng. Process 46 (2007) 119.
[35] M. Kanezashi, M. Asaeda, Hydrogen permeation characteristics and stability of Ni-doped silica membranes in steam at high temperature, J. Membr. Sci. 271 (2006) 86.
[36] S. Araki, N. Mohri, Y. Yoshimitsu, Y. Miyake, Synthesis, characterization and gas permeation properties of a silica membrane prepared by high-pressure chemical vapor deposition, J. Membr. Sci. 290 (2007) 138.
[37] T. Zivkovic, N.E. Benes, D.H.A. Blank, H.J.M. Bouwmeester, Characterization and Transport properties of surfactant-templated silica layers for membrane applications, J. Sol–Gel Sci. Technol. 31 (2004) 205.
[38] S. Gopalakrishnan, Y. Yoshino, M. Nomura, B.N. Nair, S.-I. Nakao, A hybrid processing method for high performance hydrogen-selective silica membranes, J. Membr. Sci. 297 (2007) 5.